Quantum modes on chaotic motion: Analytically exact results

Sudhir R. Jain,[1] Benoît Grémaud,[2] and Avinash Khare[3]

[1]*Nuclear Physics Division, Bhabha Atomic Research Centre, Mumbai 400094, India*
[2]*Laboratoire Kastler Brossel, Université Pierre et Marie Curie, 4 place Jussieu, 75252 Paris Cedex 05, France*
[3]*Institute of Physics, Sachivalaya Marg, Bhubaneswar 751005, India*

We discover a class of chaotic quantum systems for which we obtain some analytically exact eigenfunctions in closed form. These results have been possible due to connections shown between random matrix models, many-body theories, and dynamical systems. We believe that these results and connections will pave the way to a better understanding of quantum chaos.

PACS number(s): 05.45.Mt, 03.65.Ge

I. INTRODUCTION

Even as we understand for long that the world is quantal and buried in it is classical dynamics that is chaotic, finding eigenfunctions analytically from the the Schrödinger equation has turned out to be a near impossibility. Chaotic behavior [1,2] is characterized by the existence of positive Lyapunov exponents, which determine the rate of exponential separation of very close trajectories in the phase space of the system. Upon casting the chaotic systems in a quantum mechanical framework, impressions of chaos are found in variety of statistical properties of energy levels and eigenfunctions [3–5]. The fluctuation properties of energy level sequences of chaotic quantum systems agree very well with the results in random matrix theory [6].

Eigenfunctions and eigenvalues contain all the information about a time-independent quantum system. Chaotic eigenfunctions have been studied in detail and there are two main ideas around which the general understanding has evolved. According to Berry [7], for chaotic systems, eigenfunctions corresponding to excited states are conjectured to be well represented as a random superposition of plane waves. This conjecture has a lot of numerical support on one hand, and, is connected to statistical mechanics on the other [8,9]. The other idea ensues from Heller's discovery [10,11] of scarring of eigenfunctions by periodic orbits, where the probability density is considerably enhanced on the periodic orbit in configuration or phase space. This discovery has helped in understanding how classical periodic orbits form the underlying fabric for quantum states, and it helps in appreciating the beautiful nodal patterns and contour plots of chaotic eigenfunctions. Nevertheless, an analytical expression is not obtained, and, Berry's conjecture (which is statistical in nature) does not help in seeing how coefficients in the superposition arrange for striking patterns. Clearly, these two main ideas are not in mutual conflict.

Random matrix theory is connected in a ''magical'' way to several other topics in physics and mathematics, including complex quantum systems, Riemann zeta function, exactly solvable many-body problems, partial differential equations, and the Riemann-Hilbert problem [12,13]. These different areas are related to each other by the universal statistical properties of sequences characterizing them, such as energy levels of nuclei and chaotic quantum systems, zeros of the Riemann zeta function, and eigenvalues of transfer matrices of disordered conductors. Moreover, joint probability distribution function (JPDF) of eigenvalues of random matrices is given by a statistical mechanics problem involving particles with Coulomb-like interactions [14]. The JPDF gives the probability with which eigenvalues $\{E_i\}$ are found in intervals $[E_i, E_i + dE_i]$; all the correlation functions giving various physical quantities follow from this. These problems belong to the general class of exactly solvable statistical mechanics models. In turn, these models may be converted to problems in Hamiltonian dynamics where one can study the classical and quantal aspects.

In this paper, we extend these connections to another class of random matrix models developed to explain intermediate statistics found in pseudointegrable systems, the Anderson model in three dimensions at the metal-insulator transition point and in certain problems in atomic physics [15–18,29]. The sequences involved in these systems exhibit a behavior intermediate to regular and chaotic. Once again, the eigenvalue distribution of such random matrices is related to an exactly solvable statistical mechanics model where the interaction is a screened Coulomb-like along with an additional three-body term [19,20]. Here, the above-mentioned model is mapped into a problem in Hamiltonian dynamics in d dimensions, which is shown to display chaos. Thus, the exactly solved many-body problem is nonintegrable in the sense that there are lesser number of constants of the motion than the degrees of freedom. Quantum mechanically, thus, chaotic eigenfunctions are found analytically even though the underlying classical dynamics at the same energies is chaotic.

For quantum cat maps (toral automorphisms), analytical form for the eigenfunctions is known [21–22], where the solutions were possible because the semiclassical studies turned out to be exact.

For bringing out the connections clearly for the reader, we divide the arguments into short sections.

II. FROM A MANY-BODY PROBLEM TO A ONE-BODY PROBLEM

In 1999, a many-body problem in one dimension was discovered [19,23] where the nearest neighbors interact via a repulsive interaction that is inverse square in distance between the particles and an attractive three-body interaction,

also inverse-square in position coordinates of the particles. The N-particle problem on a circle has the Hamiltonian

$$H = \sum_{i=1}^{N} \frac{p_i^2}{2m} + g \frac{\pi^2}{L^2} \sum_{i=1}^{N} \sin^{-2}\left[\frac{\pi}{L}(x_i - x_{i+1})\right]$$
$$- G \frac{\pi^2}{L^2} \sum_{i=1}^{N} \cot\left[\frac{\pi}{L}(x_{i-1} - x_i)\right] \cot\left[\frac{\pi}{L}(x_i - x_{i+1})\right],$$

(1)

with $x_j = x_{N+j}$. In the rest of this paper, we will take the mass as unity and the circumference $L = \pi$, for notational simplicity. The potential is singular whenever $x_{j+1} = x_j + n\pi$ (n being an integer) with an inverse-square singularity. This leads to disconnected domains where the wave functions are zero at singular (hyper)planes in the quantum problem. We choose the domain in which the particles are ordered as $x_1 \leq x_2 \leq \cdots \leq x_1 + \pi$. The center-of-mass (c.m.) motion can be separated in this case by writing the amplitudes of the motion of particles around the c.m., $X = (1/N)\Sigma_{i=1}^{N} x_i$ in terms of normal mode coordinates [24]. Thus, we can write the positions as $x_j = X + y_j$, and y_j's as

$$y_j = -\frac{\pi}{2} + \left(j - \frac{1}{2}\right)\frac{\pi}{N} + \frac{1}{\sqrt{N}} q_M \cos(\pi j)$$
$$+ \left(\frac{2}{N}\right)^{1/2} \sum_{n=1}^{M-1} \left[q_n \cos\left(\frac{2\pi n j}{N}\right) - q_{-n} \sin\left(\frac{2\pi n j}{N}\right)\right]$$

(2)

for even N ($M = N/2$); and for odd N, without the last term on the right hand side and summation going upto $n = M$. The quantum Hamiltonian operator transforms to

$$H = H_{\text{c.m.}}(X) + H_{\text{billiard}}(\{q_n\})$$
$$= -\frac{1}{2N} \frac{\partial^2}{\partial X^2} - \frac{1}{2} \sum_{n}^{M} \frac{\partial^2}{\partial q_n^2} + \sum_{j=1}^{N} W[y_j(\{q_n\})], \quad (3)$$

where $W[y_j(\{q_n\})]$ is the potential term in Eq. (1). Note that $n = \pm 1, \pm 2, \ldots, \pm M$ for odd N while $n = \pm 1, \pm 2, \ldots, \pm (M-1), M$ for even N. Thus, H_{billiard} represents a single particle in an $(N-1)$-dimensional domain bounded by the (hyper)planes where potential becomes singular forcing all the wave functions to be zero on the boundaries of the domain. This gives us a class of billiards as a function of β [defined through $G = \beta^2$ and $g = \beta(\beta-1)$] and from dimensions two to $(N-1)$. A similar connection was realized by Rey and Choquard [24] when they considered the Calogero-Sutherland-Moser (CSM) system and showed that the N-body problem in this case is mapped to an integrable billiard problem in $(N-1)$ dimensions. It is interesting to note that the CSM and our model coincide for three particles as nearest neighbors are all the neighbors and the cotangent term is unity owing to a trigonometric identity. Unlike this, and most interestingly, our many-body problem leads to non-integrable billiards for particles greater than three and hence, billiards of dimension greater than two. We now turn to show
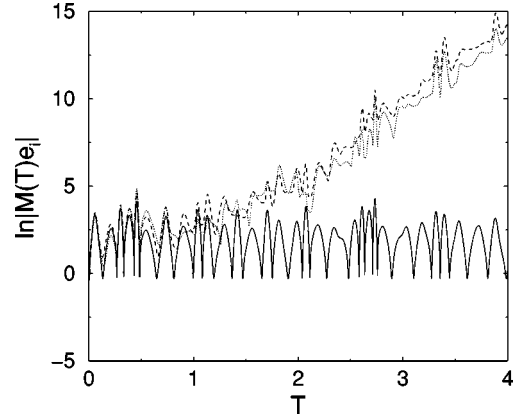

FIG. 1. $\widetilde{\lambda}^i(T) = \ln(|M(T) \cdot \mathbf{e}^i|)$, for $i = \parallel$ (continuous line), $\perp$ (dotted line), and r (dashed line), for $\beta = 2$ (see text for definition and initial conditions). As expected, $\widetilde{\lambda}^{\parallel}(T)$ is bounded, whereas $\widetilde{\lambda}^{\perp}(T)$ and $\widetilde{\lambda}^{\text{r}}(T)$ show linear behavior, emphasizing presence of hard chaos in the system.

that for $N > 3$, our billiard models are, in fact, chaotic. This also implies nonintegrability of the many-body problem.

III. FAMILY OF CLASSICAL BILLIARDS

For the sake of concreteness, we concentrate our discussion on $N = 4$, leading to a three-dimensional (3D) billiard. Equations of motion are singular each time a collision occurs (involving 2, 3, or 4 particles), but two-particle collisions are forbidden by energy conservation, giving rise to smooth integration using standard Runge-Kutta method, until one reaches a multiple collision [25]. Preliminary studies show that regularization of the classical motion near these collisions could be done, but its exact implementation has not been achieved yet. Nevertheless, we believe that this problem does not alter results presented here. For each trajectory, we have also computed the associated monodromy matrix, M (whose symplectic structure is used as a relevant test), allowing us to extract evidence of chaotic behavior in our system. For this, we have computed the "Lyapunov exponents," $\widetilde{\lambda}(T) = \ln(|M(T) \cdot \mathbf{e}_0|)$ using three different vectors: $\mathbf{e}_0^{\parallel}$, $\mathbf{e}_0^{\perp}$, and $\mathbf{e}_0^{\text{r}}$, which are, respectively, unit vector parallel to the flow at an initial time, unit vector perpendicular to the energy shell at an initial time and a "random" unit vector, namely, $1/\sqrt{6}(1,1,1,1,1,1)$. $\widetilde{\lambda}^{\parallel}(T)$, being equal to $\ln|\dot{\mathbf{X}}(T)|/|\dot{\mathbf{X}}(0)|$, is bounded entailing thereby a vanishing Lyapunov exponent, providing a reference scale for further numerical estimation of nonvanishing Lyapunov exponent. For $\beta = 2$, at classical energy equal to the quantum ground state energy $\epsilon_0 = 4\beta^2$ [see Eq. (5)], and initial conditions,

$$\begin{pmatrix} q_1(0) \\ q_{-1}(0) \\ q_2(0) \end{pmatrix} = \begin{pmatrix} 0.1 \\ 0.2 \\ 0.0 \end{pmatrix} \begin{pmatrix} p_1(0) \\ p_{-1}(0) \\ p_2(0) \end{pmatrix} = \begin{pmatrix} 1.0000 \\ 2.0000 \\ 5.1844 \end{pmatrix}, \quad (4)$$

results on Lyapunov exponents are plotted in Fig. 1. As expected, behavior of $\widetilde{\lambda}^{\parallel}(T)$ is substantially different from
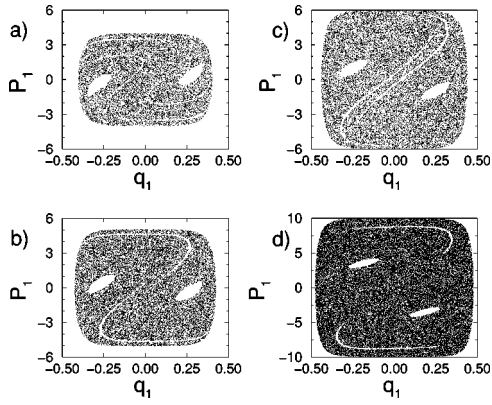
FIG. 2. Reduced PSOS defined by $q_2=0$, at different energies: $E_a=\epsilon_0=16$ [ground state energy, see Eqs. (5)], $E_b=\epsilon_1=25.5$, $E_c=\epsilon_N=36$, and $E_d=100$. The reduced dynamics is clearly chaotic. (See text for discussion about areas appearing in the PSOS.)

those of $\tilde{\lambda}^{\perp}(T)$ and $\tilde{\lambda}^{r}(T)$, emphasizing thus the presence of hard chaos in the system, with Lyapunov exponent, $\lambda \sim 6$ [26].

A more appealing evidence of hard chaos is obtained on plotting Poincaré surface of sections (PSOS). For a generic 3D time-independent system, their dimensionality (4D) makes them quite useless for visualizing. Fortunately, in our case, symmetry properties of the Hamiltonian, viz., invariance under $q_1 \leftrightarrow q_{-1}$ exchange allows us to consider the reduced phase space made of trajectories for which $q_1=q_{-1}$ and $p_1=p_{-1}$ at any time, leading thus to an effective 2D system. Figure 2 depicts, for $\beta=2$, the reduced PSOS defined by $q_2=0$, at different energies : $E_a=\epsilon_0=16$ [ground state energy, see Eq. (5)], $E_b=\epsilon_1=25.5$, $E_c=\epsilon_N=36$ [see text following Eqs. (7)–(8)], and $E_d=100$.

The empty areas appearing on all these plots correspond to trajectories having a four-body collision in their past, this has been checked by propagating the corresponding initial conditions backward in time [27]. Nevertheless the system appears to be fully chaotic in the reduced phase space, which is emphasized by the fact that all periodic orbits of the reduced dynamics are unstable (i.e., nontrivial eigenvalues of the monodromy matrix are not on the unit circle). Actually these orbits are also unstable when considered in the full phase space. Moreover, there are also unstable periodic orbits not belonging to the reduced phase space. We have also found unstable periodic orbits for which the four nontrivial eigenvalues of the monodromy matrix form a quadruplet $(\Lambda, \Lambda^*, \Lambda^{-1}, \Lambda^{-1*})$, Λ being complex.

$\beta=2$ is not a special value, we have checked that all results presented here also hold for other values $\beta > 1$.

IV. FAMILY OF QUANTUM BILLIARDS

We shall now use the known exact energy eigenstates [28] of the newly discovered N-body Hamiltonian (1) and obtain few energy eigenvalues and eigenfunctions of the corresponding $(N-1)$-dimensional billiard. The billiard eigenfunctions are obtained by eliminating the center-of-mass dependence while the eigenvalues are determined by
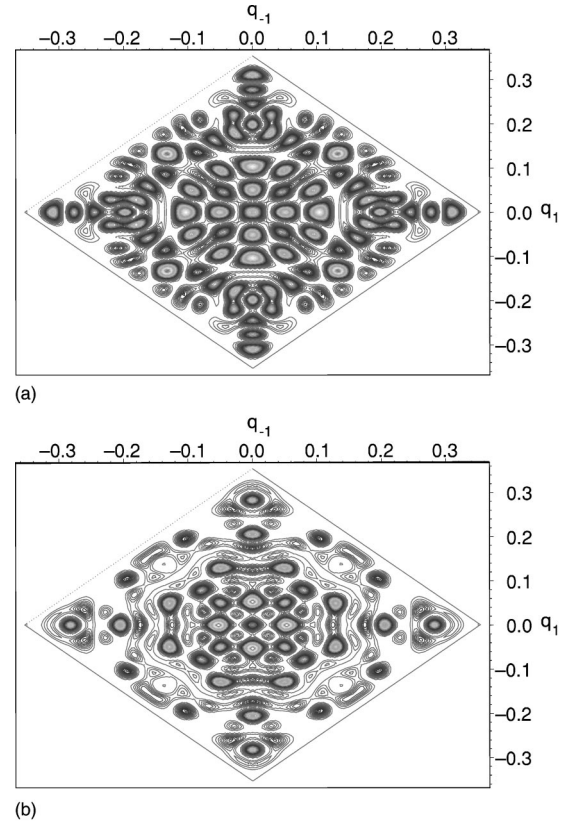

FIG. 3. Contour plots of excited states of the system with $\beta=2$ and energies (a) E = 812.5 and (b) 813.4 in the q_{-1}-q_1 plane.

subtracting off the center-of-mass energy.

Let E_k, ψ_k denote the energy eigenvalues and eigenfunctions of the N-body problem (1) with periodic boundary conditions, i.e., $H\psi_k=E_k\psi_k$. Then the exact ground state is given by [19,23]

$$\psi_0=\prod_{j}^{N} |\sin(x_j-x_{j+1})|^{\beta}, \quad E_0=N\beta^2, \quad (5)$$

provided g, G are related by $g=\beta(\beta-1), G=\beta^2$.

In addition to the ground state, a few of the excited energy eigenstates have also been obtained in this case [28] and are given by ($\psi_k=\psi_0\phi_k$),

$$\phi_1=e_1, \quad E_1=E_0+2+4\beta,$$

$$\phi_{N-1}=e_{N-1}, \quad E_{N-1}=E_0+2N-2+4\beta,$$

$$\phi_N=e_1 e_N - \frac{N}{1+2\beta}e_N, \quad E_N=E_0+2N+4+8\beta. \quad (6)$$

Here e_j $(j=1,2,\ldots,N)$ is an elementary symmetric function of order j in the variable z_j. For example $e_2=z_1 z_2+z_1 z_3+\cdots$ (containing $N(N-1)/2$ terms) and $z_j=\exp(2\iota x_j)$. Note that ϕ_k is an eigenfunction of the momentum operator with eigenvalue k [30]. Following the treatment in Ref. [24], it is easily shown that if the billiard Hamiltonian satisfies the eigenvalue equation $H_B\chi_k=\epsilon_k\chi_k$, then the ei-
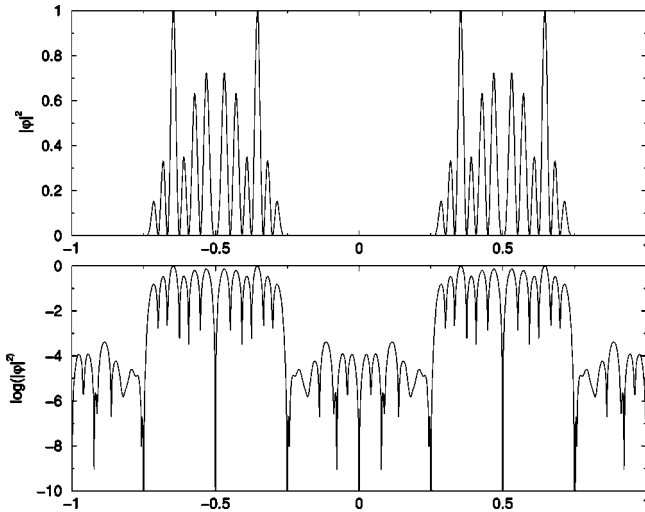
FIG. 4. The squared modulus of the excited state eigenfunction at energy $E = 812.5$ suggests some scaling properties.

FIG. 5. The Poincaré surfaces of section for the energies corresponding to the excited states shown in Fig. 3.

genvalues ϵ_k and the eigenfunctions χ_k are related to E_k, ψ_k by $\chi_k = \exp(-2\imath kX)\psi_k$ with $\epsilon_k = E_k - (2k/N)$. Finally, we then obtain the following excited eigenvalues and eigenfunctions for the $(N-1)$ billiard

$$\chi_{1c} = \psi_0 \left[\cos \frac{2}{N}([N-1]x_1 - \cdots - x_N) + \text{cyc.} \right], \quad (7)$$

$$\chi_N = \psi_0 \sum_{i<j=1}^{N} \cos 2(x_i - x_j) + \frac{N\beta}{1+2\beta}, \quad (8)$$

where E_0 is as given in Eq. (5), and cyc. is an abbreviation for "cyclic permutations." In Eq. (7), χ_{1s} is obtained by replacing cos by sin. The eigenvalues corresponding to the eigenfunctions written above are, respectively, $\epsilon_{1c} = \epsilon_{1s} = E_0 + 4\beta + 2 - (2/N)$, and, $\epsilon_N = E_0 + 8\beta + 4$. Note that even though χ_N is N dependent, the energy difference $\epsilon_N - E_0$ is N independent.

These expressions constitute the main result of the paper. The classical dynamics at energy equal to the energy eigenvalues of the eigenfunctions is chaotic, yet the eigenfunctions are analytically expressible and are not a random superposition of plane waves. However, since β can assume any value, the functions could be quite complicated, yet comprehensible. Thus, Berry's conjecture would be expectedly true for highly excited chaotic states, and not for chaotic states in general. We show here some excited states as con-
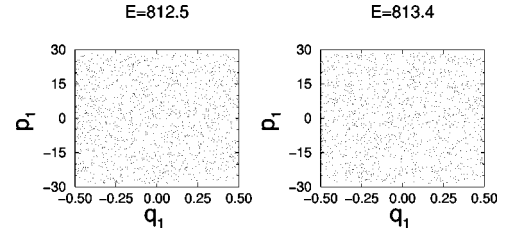
tour plots in q_{-1}-q_1 plane [Figs. 3(a) and 3(b)] at energies 812.5 and 813.4. Surprisingly, these eigenfunctions do not seem to be random; in fact, the square of the modulus of the eigenfunctions do suggest some scaling properties (Fig. 4). Whether these could be fractals is a subject of an ongoing investigation. The recent work [31] on quantum fractals may be useful in this context. In Fig. 5, the Poincaré surfaces of section show classically chaotic motion at the energies corresponding to the excited states.

We believe that chaos in quantum wave function, even at low energies, would show up as the system evolves. The time-dependent wave function, written as a superposition of eigenfunctions, has coefficients displaying chaos. Thus, eigenfunctions form an invariant set in quantum theory, much in the same way as periodic orbits and fixed points do in classical theory. The most important evidence is shown by Heller's discovery of scars. Thus, we state—scarring of wave functions on periodic orbits is a reminder of the classical fact that on its way, an arbitrary trajectory is shadowed by periodic orbits.

It is worth noting that the existence of Bose-Einstein condensation in a related one-dimensional many-body problem at zero temperature is proved recently [20]. To prove the existence of a Bose-Einstein condensate in one dimension at nonzero temperatures, we need the excited states. Thus, the development presented here is of importance to the general theory of quantum phase transitions also.

ACKNOWLEDGMENTS

[1] E. Ott, *Chaos in Dynamical Systems* (Cambridge University, New York, 1993).

[2] J.R. Dorfman, *An Introduction to Chaos in Nonequilibrium Statistical Mechanics* (Cambridge University, New York, 1999).

[3] M.C. Gutzwiller, Am. J. Phys. **66**, 304 (1997).

[4] M.C. Gutzwiller, *Chaos in Classical and Quantum Physics* (Springer-Verlag, New York, 1990).

[5] D. Delande, D. Sornette, and R.L. Weaver, J. Acoust. Soc. Am. **96**, 1873 (1994).

[6] T. Guhr, A. Müller-Groeling, and H.A. Weidenmüller, Phys. Rep. **299**, 189 (1998).

[7] M.V. Berry, J. Phys. A **10**, 2083 (1977).

[8] M. Srednicki, Phys. Rev. E **50**, 888 (1994).

[9] S.R. Jain and D. Alonso, J. Phys. A **30**, 4993 (1997).

[10] E.J. Heller, Phys. Rev. Lett. **53**, 1515 (1984).

[11] L. Kaplan, Nonlinearity **12**, R1 (1999).

[12] L.P. Kadanoff, Phys. Today **(53)**, 11 (2000).

[13] P. Deift, *Orthogonal Polynomials and Random Matrices*: *A Riemann-Hilbert Approach*, Courant Lecture Notes in Mathematics, Vol. 3 (American Mathematical Society, Providence, Rhode Island, 2000).

[14] M.L. Mehta, *Random Matrices*, 2nd ed. (Academic, London, 1991).

[15] B. Grémaud and S.R. Jain, J. Phys. A **31**, L637 (1998).

[16] B. Shklovskii, B. Shapiro, B.R. Sears, P. Lambradines, and H.B. Shore, Phys. Rev. B **47**, 11 487 (1993).

[17] G. Date, S.R. Jain, and M.V.N. Murthy, Phys. Rev. E **51**, 198 (1995).

[18] E. Bogomolny, U. Gerland, and C. Schmit, Phys. Rev. E **59**, R1315 (1999).

[19] S.R. Jain and A. Khare, Phys. Lett. A **262**, 35 (1999).

[20] G. Auberson, S.R. Jain, and A. Khare, Phys. Lett. A **267**, 293 (2000).

[21] B. Eckhardt, J. Phys. A **19**, 1823 (1986).

[22] J.P. Keating, Nonlinearity **4**, 309 (1991).

[23] G. Auberson, S.R. Jain, and A. Khare, J. Phys. A **34**, 695 (2001).

[24] S. Rey and P. Choquard, Eur. J. Phys. **18**, 94 (1997).

[25] Occurrences of the latter case are systematically checked in our code and the corresponding trajectories are discarded.

[26] From a numerical point of view, one should mention that the present trajectory alone can be followed up to time $T \sim 80$ without trouble and also that at $T = 4$, the symplectic structure has been preserved better than 10^{-8} (relative). Of course, these behaviors are not qualitatively modified on changing either initial conditions or energy.

[27] More precisely, trajectories having initial conditions in the two largest areas will perform the collision (backward in time) before returning to PSOS, whereas other areas are images of these largest areas by the Poincaré map (backward in time).

[28] M. Ezung, N. Gurappa, A. Khare, and P.K. Panigrahi, e-print cond-mat/0007005.

[29] H.D. Parab and S.R. Jain, J. Phys. A **29**, 3903 (1996).

[30] $-2 p_k \equiv 2\iota \partial/\partial x = z_k \partial/\partial z_k$.

[31] D. Wojcik, I. Bialynicki-Birula, and K. Zyczkowski, Phys. Rev. Lett. **85**, 5022 (2000).